

# Automated optimization of an aspheric light-emitting diode lens for uniform illumination

Xiaoxia Luo,<sup>1,2</sup> Hua Liu,<sup>1,\*</sup> Zhenwu Lu,<sup>1</sup> and Yao Wang<sup>1</sup>

<sup>1</sup>Opto-electronics Technology Center, Changchun Institute of Optics, Fine Mechanics and Physics, Chinese Academy of Sciences, Changchun, Jilin 130033, China

<sup>2</sup>Graduate School of the Chinese Academy of Sciences, Beijing 100039, China

\*Corresponding author: liuhua\_rain@yahoo.com.cn

Received 21 March 2011; revised 4 May 2011; accepted 9 May 2011;  
posted 16 May 2011 (Doc. ID 144471); published 1 July 2011

In this paper, an automated optimization method in the sequential mode of ZEMAX is proposed in the design of an aspheric lens with uniform illuminance for an LED source. A feedback modification is introduced in the design for the LED extended source. The user-defined merit function is written out by using ZEMAX programming language macros language and, as an example, optimum parameters of an aspheric lens are obtained via running an optimization. The optical simulation results show that the illumination efficiency and uniformity can reach 83% and 90%, respectively, on a target surface of 40 mm diameter and at 60 mm away for a 1 × 1 mm LED source. © 2011 Optical Society of America  
*OCIS codes:* 080.4298, 220.2945, 230.3670.

## 1. Introduction

Compared with conventional light sources, LED light sources have many advantages for general lighting, such as longer lifetime, lower power consumption, smaller size, and safety. However, a nonuniform circular spot on the target plane will be formed when it is used for lighting directly. To solve this problem, auxiliary optical elements are often employed to redistribute the light of an LED to generate uniform illumination on the target plane.

At present, the free-form surface is mostly used in the optical design for LED lighting to achieve desired uniform illumination. There are many reports about the methods of free-form lens design [1,2]. One is the trial and error method [3–6]. Designers can modify parameters interactively until a satisfactory pattern is obtained. Nevertheless, it is very time-consuming and needs lots of special expertise. Another method is numerical solutions [7–10]. A set of vector equations, including the law of refraction, curvature of surface equation, initial conditions, etc., need to be

established with this method. It is very complicated and challenging to solve such differential equations.

In order to make the design more convenient, in this paper the two methods mentioned above are combined effectively. An automated optimization method based on macro-optimization in the sequential mode of ZEMAX is introduced for LED uniform illumination. In general, systems in the sequential mode usually outperform the system in nonsequential mode optimization, and the execution of a macro during optimization is extremely fast. Also, ZEMAX programming language macros are well-integrated within ZEMAX and require little programming experience.

First, we deduce the relationships between the location of light rays on the target plane and the incident angle according to the conservation of energy. Second, merit function (MF) is defined by comparing the locations of rays on the target plane determined via the ray-tracing method and numerical solution, which is modified by employing feedback function for an extended source. Finally, as an example, optimization is performed in sequential mode of ZEMAX with the optimization operands defined through use of the macros. One can control the incident angle of

light to any desired location and obtain the expected uniform distributions. What's more, this approach makes the design process feasible for LED extended source.

## 2. Aspheric Lens Design

The aspheric lens design is discussed and the equations required are deduced in this section. The method can be used for any source if only the source intensity distribution is given out. In this paper, in order to simplify the mathematical calculation, the LED source is assumed to be a standard Lambertian source.

### A. Optical Structure

The structure of the proposed free-form surface lens is assumed to be rotationally symmetric in the design of a combined reflective-refractive configuration. The lens model, in a two-dimensional space, is shown in Fig. 1. The angle  $\theta_c$  divides the lens into two parts, with the total internal reflection (TIR) part located outside the dash line and the refraction part inside the dash line. The TIR part consists of three optical surfaces including a free-form surface on the rear of the lens of ②, a TIR side surface of ④, and a free-form refractive surface in the out part of the front of ⑤, where rays undergo a TIR from the side surface and refractions at two refractive surfaces. While the light in the refraction part (inside the  $\theta_c$  angle) goes directly through the lens, two optical surfaces are involved, a plane surface of ① and a common convex surface of ⑥. To simplify the fabrication and reduce cost, all of the free-form surfaces of the lens are designed to be even aspheric surfaces.

### B. Optimization Theory

#### 1. Conservation of Energy

The light source is assumed to be an ideal point source. The intensity distribution of the LED source is approximate as follows [11,12]:

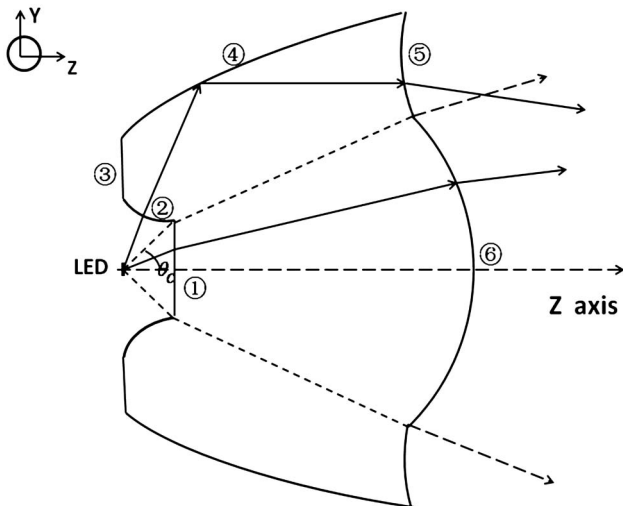


Fig. 1. Framework of the optical module.

$$I(\theta) = I_0 \cos \theta, \quad (1)$$

where  $\theta$  is the angle between the ray and the  $z$  axis, and  $I_0$  is the luminous intensity in the  $z$  axis. The total luminous flux is shown as

$$\Phi_{\text{total}} = \int I(\theta) d\Omega = \pi I_0 \sin^2 \theta_{\text{max}}. \quad (2)$$

In our case, we need a uniform irradiance, that is, the illuminance on the target plane is constant, then we have  $E(y) = E_0$ . Accordingly, we have

$$\Phi'_{\text{total}} = \int_0^{R_{\text{max}}} E(y) \cdot 2\pi y dy = E_0 \cdot S. \quad (3)$$

Here,  $\Phi'_{\text{total}}$  is the total luminous flux on the target plane and  $S$  is the area of the target plane.

Thus, energy conservation of a lossless optical system can be expressed as follows:

$$\Phi'_{\text{total}} = \Phi_{\text{total}}. \quad (4)$$

From the above analysis, we conclude that uniform illumination means that the luminous flux of the assigned plane is proportional to the corresponding area.

#### 2. Theory of Numerical Computing Method

We assume the total luminous flux of the LED in refraction and TIR part as  $\Phi_1$  and  $\Phi_2$ , respectively, the critical angle between the two parts is  $\theta_c$ , and the corresponding incident angle is assumed as  $\theta_i$ . The initial parameter of  $\theta_c$  is important for the system, and the corresponding energy distribution will vary as  $\theta_c$ . But the theory of numerical computing MF is consistent.

1. Consideration of the refraction part where  $\theta_i$  is at  $0 \sim \theta_c$ .

First, we divide the luminous flux of the LED source in the refraction part into  $n$  equal parts. Then, each portion of the energy can be expressed as Eq. (5):

$$\phi_i = \frac{1}{n} \Phi_1 = \frac{1}{n} \pi I_0 \sin^2 \theta_c, \quad i = 1, 2, 3 \dots n. \quad (5)$$

Otherwise,

$$\begin{aligned} \phi_i &= \int_0^{2\pi} \int_{\theta_{i-1}}^{\theta_i} I_0 \cos \theta \sin \theta d\theta d\varphi \\ &= \pi I_0 (\sin^2 \theta_i - \sin^2 \theta_{i-1}), \\ \theta_0 &= 0, \quad i = 1, 2, 3 \dots n. \end{aligned} \quad (6)$$

From Eqs. (5) and (6), the incident angle per part can be written as

$$\theta_i = \sin^{-1} \left[ \left( \frac{i}{n} \right)^{1/2} \cdot \sin \theta_c \right], \quad i = 1, 2, 3 \dots n. \quad (7)$$

Second, we analyze concretely the ray's behavior in this part, where the light rays emitted from the LED enter the lens directly. On one hand, the fractional area within a circle of radius  $y_i$  is simply  $(y_i^2/R^2)$ . Here,  $R$  is the radius of the target plane, as shown in Fig. 2.

On the other hand, the light ray coming out from the source into a cone-shaped solid angle with a divergence half-angle of  $\theta_i$  has a fractional flux [11] of  $(\sin^2 \theta_i / \sin^2 \theta_c)$ ; hence, we have  $\frac{y_i^2}{R^2} = \frac{\sin^2 \theta_i}{\sin^2 \theta_c}$ . That is,

$$y_i = R \cdot \frac{\sin \theta_i}{\sin \theta_c}, \quad i = 1, 2, 3 \dots n, \quad (8)$$

where  $\theta_i$  is determined by Eq. (7).

2. Consideration of the TIR part where  $\theta_i$  is at  $\theta_c \sim \theta_{\max}$ .

Similarly, we divide the luminous flux of the LED source in the TIR part into  $n$  equal parts. Each portion of the energy is

$$\phi_i = \frac{1}{n} \Phi_2 = \frac{1}{n} \pi I_0 (\sin^2 \theta_{\max} - \sin^2 \theta_c), \quad (9)$$

$$i = 1, 2, 3 \dots n.$$

Otherwise,

$$\phi_i = \pi I_0 (\sin^2 \theta_i - \sin^2 \theta_{i-1}), \quad \theta_0 = \theta_c, \quad (10)$$

$$i = 1, 2, 3 \dots n.$$

According to Eqs. (9) and (10), the incident angle per portion in the TIR part can be expressed as

$$\theta_i = \sin^{-1} \left[ \left( \frac{i}{n} \cdot \sin^2 \theta_{\max} + \frac{n-i}{n} \cdot \sin^2 \theta_c \right)^{1/2} \right], \quad (11)$$

$$i = 1, 2, 3 \dots n.$$

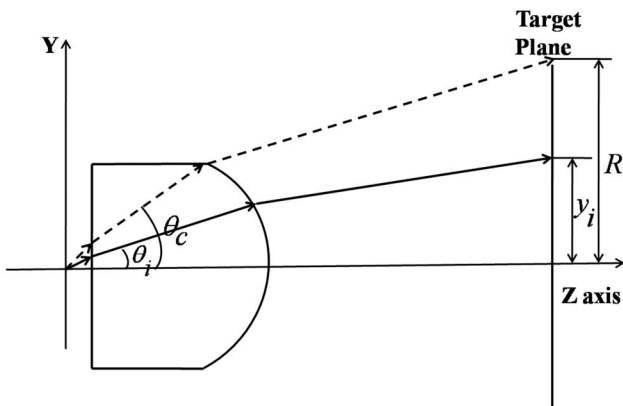


Fig. 2. Simple model of the refraction part.

In the TIR part, we assume that the rays with a divergence half-angle of  $\theta_{\max}$  will experience a TIR, refract at the refraction surfaces, and reach the center of the target plane. In contrast, the rays with the divergence half-angle of  $\theta_c$  will finally reach the boundary of the target plane. The fractional area within a circle of radius  $y_i$  is also as  $(y_i^2/R^2)$ , as shown in Fig. 3.

The corresponding rays emitted from the LED, with the divergence half-angle range from  $\theta_i$  to  $\theta_{\max}$ , have a fractional flux of  $[(\sin^2 \theta_{\max} - \sin^2 \theta_i) / (\sin^2 \theta_{\max} - \sin^2 \theta_c)]$ .

Accordingly, we have  $\frac{y_i^2}{R^2} = \frac{\sin^2 \theta_{\max} - \sin^2 \theta_i}{\sin^2 \theta_{\max} - \sin^2 \theta_c}$ .

The relation between the target radius  $y_i$  and the incident angle  $\theta_i$  is expressed as

$$y_i = R \cdot \left( \frac{\sin^2 \theta_{\max} - \sin^2 \theta_i}{\sin^2 \theta_{\max} - \sin^2 \theta_c} \right)^{1/2}, \quad i = 1, 2, 3 \dots n, \quad (12)$$

where  $\theta_i$  is determined by Eq. (11)

3. Evaluation of the efficiency and uniformity.

In fact, not only the efficiency, but also the uniformity, can be evaluated through the target radius. With Eqs. (7), (8), (11), and (12), we can deduce the relationships between each portion of the energy and the corresponding coordinates of the target plane:

$$\begin{cases} \phi_i = \frac{\Phi_1}{R^2} \cdot \frac{y_i^2}{i} & (\theta_i \leq \theta_c) \\ \phi_i = \frac{\Phi_2}{R^2} \cdot \frac{y_i^2}{n-i} & (\theta_i > \theta_c) \end{cases}. \quad (13)$$

The efficiency of each part of the system can be expressed as follows:

$$\begin{cases} \eta_1 = \frac{\Phi_{\text{image}}}{\Phi_1} = \frac{1}{\Phi_1} \cdot \sum_i \phi_i = \frac{1}{R^2} \sum_i \frac{y_i^2}{i} & (\theta_i \leq \theta_c) \\ \eta_2 = \frac{\Phi_{\text{image}}}{\Phi_2} = \frac{1}{\Phi_2} \cdot \sum_i \phi_i = \frac{1}{R^2} \sum_i \frac{y_i^2}{n-i} & (\theta_i > \theta_c) \end{cases}, \quad (14)$$

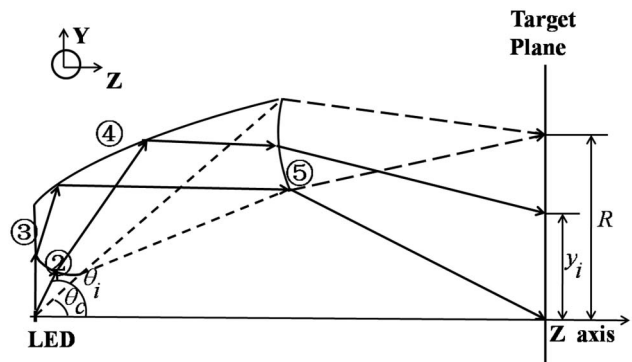


Fig. 3. Simple model of the TIR part.

so, the total efficiency of the system is

$$\eta = \frac{\eta_1 \cdot \Phi_1 + \eta_2 \cdot \Phi_2}{\Phi_1 + \Phi_2}. \quad (15)$$

Spatial uniformity [13] is defined as the relative standard deviation (RSD) of illuminance at the target plane. For a discrete set of  $n$ , illuminance values  $E_i$  is given by

$$\text{RSD} = \frac{\sigma}{E} = \sqrt{\frac{1}{n} \cdot \sum_{i=1}^n \left( \frac{E_i}{E} - 1 \right)^2}. \quad (16)$$

According to the equal divided energy and area of the target plane, we have

$$\begin{cases} \text{RSD}_1 = \sqrt{\frac{1}{n} \cdot \sum_{i=1}^n \left( \frac{iR^2}{ny_i^2} - 1 \right)^2} & (\theta_i \leq \theta_c) \\ \text{RSD}_2 = \sqrt{\frac{1}{n} \cdot \sum_{i=1}^n \left( \frac{(n+i)R^2}{ny_i^2} - 1 \right)^2} & (\theta_i > \theta_c) \end{cases}. \quad (17)$$

The uniformity of the system can be expressed as

$$\text{RSD} = \frac{\text{RSD}_1 + \text{RSD}_2}{2}. \quad (18)$$

### 3. Ray Tracing and Defining the MF

In ZEMAX, there are two forms of ray tracing, which are sequential and nonsequential ray tracing. Nonsequential ray tracing implies that there is no predefined sequence of surfaces which rays that are being traced must hit. Rays may hit any part of any nonsequential object, and may hit the same object multiple times, or not at all. This can be contrasted with sequential ray tracing, where all of the rays traced must propagate through the same set of surfaces in the same order. In sequential mode in ZEMAX, all ray propagation occurs through surfaces which are located using a local coordinate system. As for sequential ray-tracing routines, we must specify the normalized field coordinates  $h_x, h_y$  and the normalized pupil coordinates  $p_x, p_y$  to trace a particular ray through the lens system in ZEMAX. Considering the case of a point source, as shown in Fig. 4,

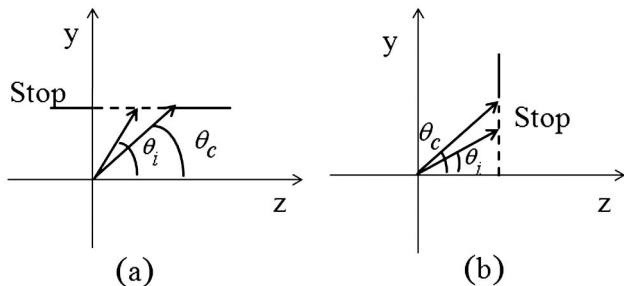


Fig. 4. Sketch of the incident angle, (a)  $\theta_i > \theta_c$  and (b)  $\theta_i \leq \theta_c$ .

the coordinates of the  $i$ th ray can be expressed as Eq. (19).

$$\begin{cases} h_x = 0, & h_y = 0 \\ p_x = 0, & p_y(i) = \frac{\theta_i}{\theta_{\max}}, \end{cases} \quad (19)$$

where  $\theta_i$  is expressed as Eq. (20):

$$\begin{cases} \theta_i = \sin^{-1} \left[ \left( \frac{i}{n} \right)^{1/2} \cdot \sin \theta_c \right], & (\theta_i \leq \theta_c) \\ \theta_i = \sin^{-1} \left[ \left( \frac{i}{n} \cdot \sin^2 \theta_{\max} + \frac{n-i}{n} \cdot \sin^2 \theta_c \right)^{1/2} \right], & (\theta_i > \theta_c) \end{cases}, \quad (20)$$

$i = 1, 2, 3 \dots n.$

According to Eqs. (8), (12), and (19), we have

$$\text{MF} = \sum_{i=1}^n (y_i - y'_i)^2, \quad (21)$$

where  $y'_i$  is the actual position of the ray on the target plane through ray tracing of the  $i$ th ray, and  $y_i$  is determined by Eq. (8) and (12) for different parts, respectively. With the MF defined by Eq. (21), we will set certain variables of lens parameters, adopt the damped least squares algorithm, which is a powerful search method, and run optimization in ZEMAX. A small MF can correspond to higher light efficiency and higher irradiance uniformity, and the optimization method does help us to drive the lens profile to fit the optimal design target more closely.

### 4. Feedback for Extended Source

Uniform illumination can be obtained with a theoretical point source. However, in the illuminance distribution appears obvious peaks and dips with extended source. One way to solve this problem is to redistribute the projected solid angle of the illuminating beam at those points to ensure the uniformity on the basis of the illuminance distribution. To be more distinct for extended source, the subscript  $i$  is replaced by  $j$ , which is just a different indication of the expression method. That is the energy mentioned previously in a given ray expressed as  $\phi_j$ . The energy acquired with extended source is expressed as  $\phi'_j$ . According to Eqs. (5) and (6), we obtain

$$\phi_j = \pi I_0 \cdot \frac{\sin^2 \theta_j}{j}, \quad j = 1, 2, 3 \dots n. \quad (\theta_j \leq \theta_c), \quad (22)$$

where  $n$  is the same as the previous mentioned.

Similarly, from Eqs. (9) and (10), we have

$$\begin{aligned} \phi_j &= \pi I_0 \cdot \frac{\sin^2 \theta_j - \sin^2 \theta_c}{j}, \\ j &= 1, 2, 3 \dots n. \quad (\theta_j > \theta_c). \end{aligned} \quad (23)$$

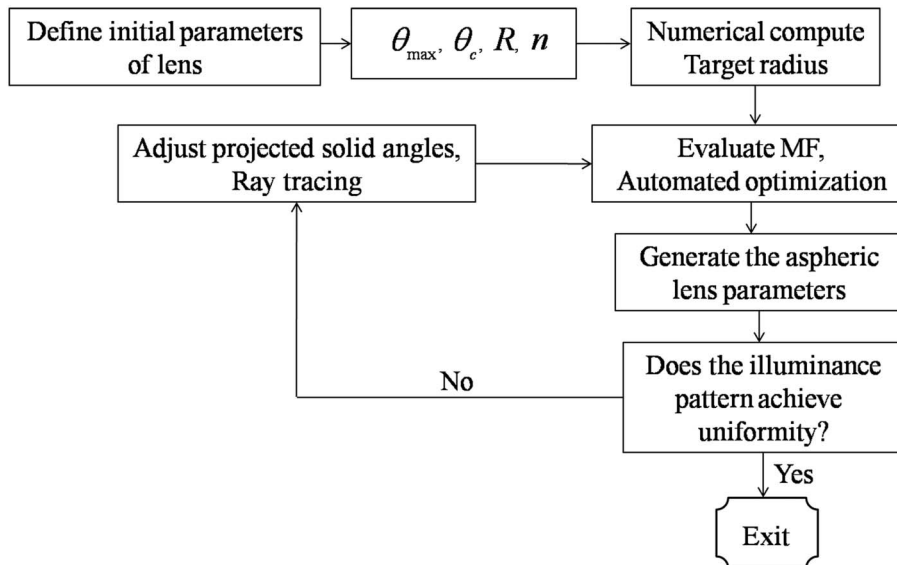


Fig. 5. Flow chart to clarify the free-form surface lens design with extended source.

By employing the feedback modification method [14], the given illuminance distribution is modified through the feedback function of  $\rho_j = \phi'_j / \phi_j$ , where  $\rho_j$  defines the fraction of each portion of energy from which the data is adjusted. To obtain the uniform illumination,  $\phi'_j$  should satisfy

$$\phi'_j = \frac{1}{\rho_j} \cdot \phi_j. \quad (24)$$

After substituting Eqs (22) and (23) into Eq. (24), respectively, Eq. (20) can be changed to

$$\begin{cases} \theta'_j = \sin^{-1} \left[ \left( \frac{1}{\rho_j} \right)^{1/2} \cdot \sin \theta_j \right], & (\theta_j \leq \theta_c) \\ \theta'_j = \sin^{-1} \left[ \left( \frac{1}{\rho_j} \cdot \sin^2 \theta_j + \frac{\rho_j - 1}{\rho_j} \cdot \sin^2 \theta_c \right)^{1/2} \right], & (\theta_j > \theta_c) \end{cases},$$

$j = 1, 2, 3 \dots n.$

(25)

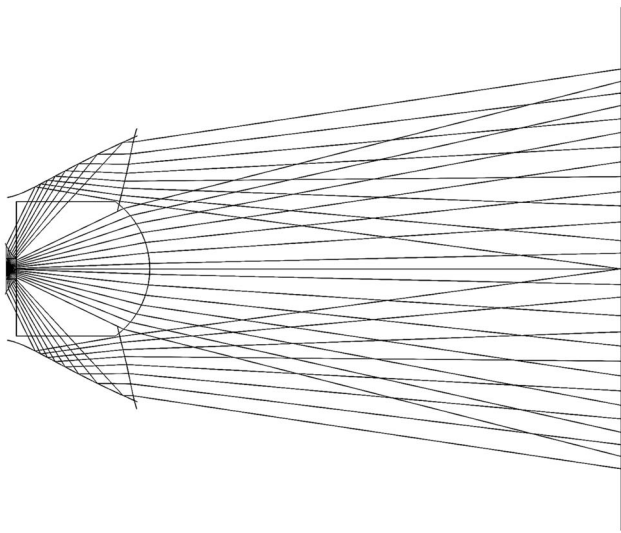


Fig. 6. Layout of the model used for free-form lens design.

For now, the key is to figure out which parts of the solid angle that illuminate the point. The energy is reapportioned within an adjacent solid angle according to the illuminance distribution. The solid angle adjusted affects only the normalized pupil coordinates of ray tracing in ZEMAX in uniform illumination.

As for extended source, the normalized pupil coordinate of  $p_y$  is transformed into

$$p_y(j) = \frac{\theta'_j}{\theta_{\max}}, \quad j = 1, 2, 3 \dots n, \quad (26)$$

where  $\theta'_j$  is determined by Eq. (25).

This optimization process is detailed in Fig. 5.

### 3. Optical Simulation Results

As an example, an aspheric lens is optimized for uniform illuminance of an LED in just a few minutes of optimization. A Lambertian source with the maximum divergence half-angle of  $90^\circ$  is used, and the critical angle is  $45^\circ$ . The illuminated target surface is a circle plane with a radius of 20 mm at the distance of 60 mm, and the material of the lens is PMMA. The

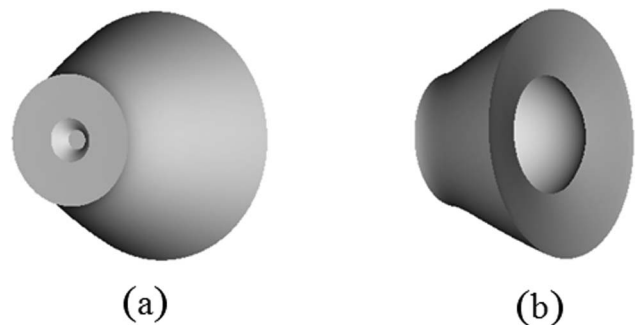


Fig. 7. Views of the optimized free-form lens design. (a) Back view and (b) front view.

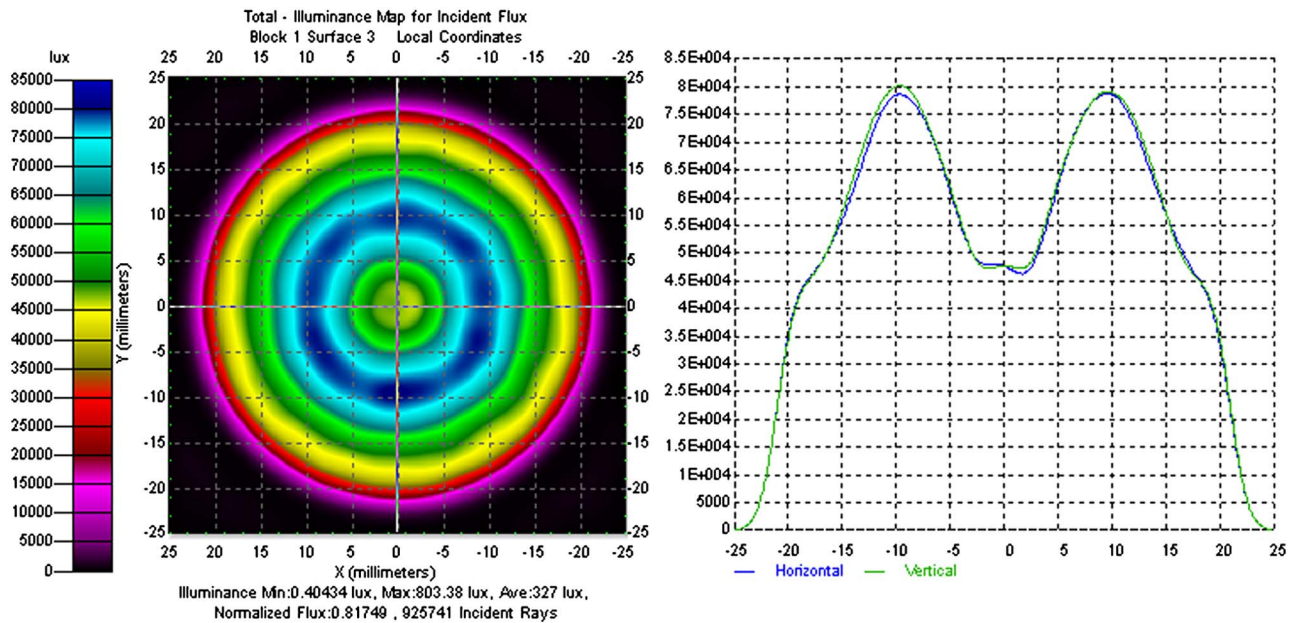


Fig. 8. (Color online) Illuminance pattern generated with the initial lens.

lens parameters, such as the radius of curvature, conic coefficients, and aspheric coefficients, are defined as variables, and cycles of optimization are set as automatic. A value of zero is ideal for the MF so that the optimization algorithm will attempt to make the value of the function as small as possible. Macros, which are user defined MF's, are written in ZEMAX's Merit Function Editor.

Optimization takes 47 min on a dual-processor computer and requires approximately 1500 cycles of the MF, whereas nonsequential optimization requires several hours or even several days. Optimization in the sequential mode for illumination optics is an approximation method, which is more simple and

fast in the design of nonimaging optics compared with numerical solutions. The lens achieves better performance within the permitted scope of precision. The layout of the designed lens in ZEMAX's multiple configurations is shown in Fig. 6. Stray light and a black hole may occur between the TIR and refractive parts in the multiconfiguration of the system. However, it has very little effect on the illumination of the lens through analysis in the nonsequential mode of ZEMAX where the lens obtained in the sequential mode is imported.

The TracePro software package is used to simulate and verify the optical performance of this aspheric lens. The profile of the optimized aspheric lens is

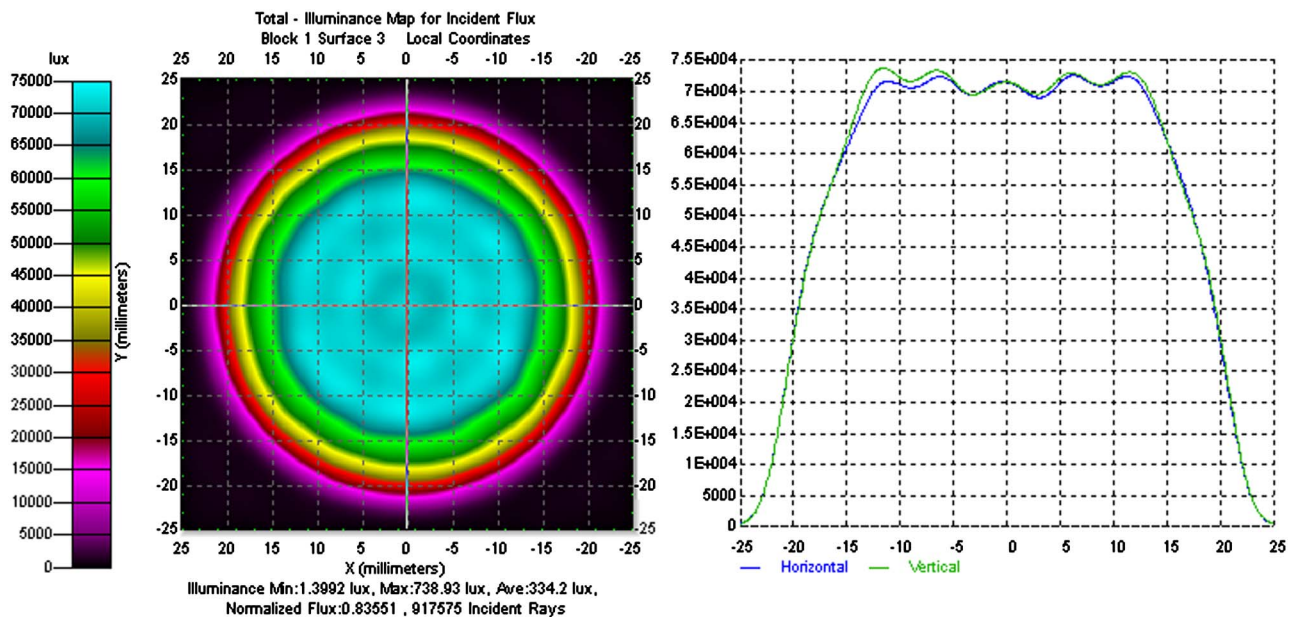


Fig. 9. (Color online) Illuminance pattern generated with the optimized lens.

depicted in Fig. 7. In the simulation, an extended Lambertian emitting surface with an emitting area of  $1\text{ mm} \times 1\text{ mm}$  is used as extended source, and 1 million light rays are traced to verify the feasibility of this method. Both Fresnel losses and absorption losses are considered. Figures 8 and 9 show the simulation results of the illumination systems with the original and the optimized lens profile, respectively.

It can be seen in Fig. 8 that the illuminance distribution is bad, with the light transfer efficiency about 81% and the uniformity of only 60%. Here, uniformity is defined as the ratio of the minimum to the maximum illuminance on the target plane. It is shown in Fig. 9 that the light transfer efficiency is 83%, and the uniformity across the center is near 90% which is quite good. The illumination on the outer of the circle is a little lower compared with the center, according to Fig. 9. This is caused by the absorptions of the black hole between the TIR and refractive parts of the aspheric lens. By comparing Figs. 8 and 9, it can be found that the illumination uniformity increases by 30% after optimization. The simulation results demonstrate the feasibility of this method for extended the LED source.

#### 4. Conclusions

In this study, in order to achieve uniform illumination of LEDs, the method of automated optimization for designing an aspheric lens is proposed. The theory of edit of user-defined MF has been discussed in detail. A feedback modification is introduced in the design for an LED extended source. Optimum lens parameters, which are variables in the optimization, are obtained with this method. The simulation results indicate that it is an effective method to generate uniform illumination for an LED extended source. A uniformity of 90% and an optical efficiency of 83% with an LED chip of size  $1 \times \text{mm} \times 1\text{ mm}$  is achieved. This design method is also applicable to other sources by taking the actual distribution of the source intensity into account. Although the illumination on the target plane still needs to be improved to meet the illumination requirement in a real projection system, this design approach really

reduces the difficulty of lens design and attains better performances.

The work described in this paper is supported by the National Basic Research Program of China with grant 2010CB227101 and by the Innovation Program of the Chinese Academy of Sciences.

#### References

1. B. Parkyn and D. Pelka, "Free-form illumination lenses designed by a pseudo-rectangular lawnmower algorithm," *Proc. SPIE* **6338**, 633808 (2006).
2. L. Wang, "Discontinuous free-form lens design for prescribed irradiance," *Appl. Opt.* **46**, 3716–3723 (2007).
3. J. Bortz, N. Shatz, and D. Pitou, "Optimal design of a nonimaging projection lens for use with an LED source and a rectangular target," *Proc. SPIE* **4092**, 130–138 (2000).
4. B. A. Jacobson and R. D. Gengelbach, "Lens for uniform LED illumination: an example of automated optimization using Monte Carlo ray-tracing of an LED source," *Proc. SPIE* **4446**, 121–128 (2001).
5. S. Kudaev and P. Schreiber, "Automated optimization of non-imaging optics for luminaires," *Proc. SPIE* **5962**, 59620B (2005).
6. W. Z. Zhang, Q. X. Liu, H. F. Gao, and F. H. Yu, "Free-form reflector optimization for general lighting," *Opt. Eng.* **49**, 063003 (2010).
7. H. Ries, "Tailored freeform optical surfaces," *J. Opt. Soc. Am. A* **19**, 590–595 (2002).
8. H. Ries and J. Muschaweck, "Tailoring freeform lenses for illumination," *Proc. SPIE* **4442**, 43–50 (2001).
9. Y. Ding, X. Liu, Z. R. Zheng, and P. F. Gu, "Freeform LED lens for uniform illumination," *Opt. Express* **16**, 12958–12966 (2008).
10. Y. Ding and P. F. Gu, "Freeform reflector for uniform illumination," *Acta Optica Sinica* **27**, 540–544 (2007).
11. Z. R. Zheng, X. Hao, and X. Liu, "Freeform surface lens for LED uniform illumination," *Appl. Opt.* **48**, 6627–6634 (2009).
12. F. Chen, S. Liu, K. Wang, Z. Y. Liu, and X. B. Luo, "Free-form lenses for high illumination quality light-emitting diode MR16 lamps," *Opt. Eng.* **48**, 123002 (2009).
13. F. Fournier and J. Rolland, "Optimization of freeform light-pipes for light-emitting-diode projectors," *Appl. Opt.* **47**, 957–966 (2008).
14. Y. Luo, Z. X. Feng, Y. J. Han, and H. T. Li, "Design of compact and smooth free-form optical system with uniform illuminance for LED source," *Opt. Express* **18**, 9055–9063 (2010).